European Polymer Journal 118 (2019) 290–305

Contents lists available at ScienceDirect

European Polymer Journal

journal homepage: www.elsevier.com/locate/europolj

Preparation and characterization of chemical grouting derived from lignin epoxy resin

Yingtuan Zhang[a,b], Hao Pang[a], Daidong Wei[a], Jialin Li[a,b], Simin Li[a,b], Xiuju Lin[a,b], Fei Wang[d,e], Bing Liao[a,c,*]

[a] Guangzhou Institute of Chemistry, Chinese Academy of Sciences, Guangzhou 510650, China
[b] University of Chinese Academy of Sciences, Beijing 100049, China
[c] Guangdong Academy of Sciences, Guangzhou 510650, China
[d] Guangdong Province Key Laboratory of Industrial Surfactant, Guangzhou 510665, China
[e] Guangdong Research Institute of Petrochemical and Fine Chemical Engineering, Guangzhou 510665, China

ARTICLE INFO

Keywords:
Lignin valorization
Grouting materials
Epoxy resin
Quantitative NMR spectroscopy
Mechanical test
Bio-based thermoset

ABSTRACT

Lignin was used herein to prepare chemical grouting materials as replacements for petroleum-based epoxy precursors. Demethylation, phenolation, and hydroxymethylation were conducted and the products were characterized via FT-IR, ^{1}H NMR, and GPC. A quantitative NMR method was used to study the precise changes in the functional group composition. Raw lignin (RL), demethylated lignin (DML), phenolated lignin (PHL), and hydroxymethylated lignin (HML) were respectively reacted with epichlorohydrin to synthesize various lignin epoxy resin (LEP), including raw lignin epoxy resin (RLEP), demethylated lignin epoxy resin (DMLEP), phenolated lignin epoxy resin (PHLEP), and hydroxymethylated lignin epoxy resin (HMLEP). With LEP as feedstocks, new grouting materials were prepared and the effects of the RLEP content and the LEP variants were investigated. The results demonstrated that the prepared lignin epoxy grouting resin had outstanding viscosity and mechanical properties with RLEP content up to 16%, and this performance greatly exceeded the industry standard. DMLEP, PHLEP, and HMLEP were able to provide better tensile properties, heat-resistance, chemical-resistance and curing performance compared with that achieved with RLEP. Overall, lignin has displayed great potential in replacing petroleum-based materials for the preparation of high-performance chemical grouting materials.

1. Introduction

Grouting has been widely used in seepage prevention, strength reinforcement, leakage plugging, and waterproofing since the early eighteenth century [1]. In 1887, a two-component sodium silicate slurry was invented as the first chemical grouting material and began to take the place of its traditional clay or cement counterparts. In contrast with a particle-containing slurry such as clay or cement material, a chemical grouting material is a molecular solution with extra low viscosity, great grouting performance, and possesses excellent strength after consolidation.

Epoxy resins have outstanding potential as grouting materials, as they possess superior strength, fine adhesion performance, low contraction, and they can be prepared as tunable formulations. However, more than 90% of the production of epoxy resins worldwide has been conducted via condensation reactions involving bisphenol A (BPA), which has been generally considered to be a toxic and environmentally harmful material [2]. Medical research has shown that BPA behaves as an analog of estrogen when it is ingested into the human body [3], and thus can cause embryotoxicity as well as teratogenicity [4]. With this in mind, researchers have devoted many efforts toward synthesizing epoxy resins from bio-based alternatives rather than BPA. Consequently, epoxy prepolymers have been synthesized from other feedstocks, such as epoxidized cardanol [5], isosorbide [6], gallic acid [3], tannins [7], and vegetable oil [8].

Among these bio-based alternatives, lignin s an ideal candidate due to its natural aromatic structure. As one of the most abundant natural bio-resources, lignin is an underutilized byproduct of the forestry industry [9]. Nearly 50 million tons of lignin are produced each year, but only 2% are used for the production of value-added materials [10]. Still, the abundance and economic efficiency of lignin have made it a promising renewable ingredient for various applications. Lignin is

* Corresponding author at: Guangzhou Institute of Chemistry, Chinese Academy of Sciences, Guangzhou 510650, China.
E-mail address: liaobing@gic.ac.cn (B. Liao).

https://doi.org/10.1016/j.eurpolymj.2019.05.003
Received 1 March 2019; Received in revised form 18 April 2019; Accepted 3 May 2019
Available online 03 May 2019
0014-3057/

typically a three-dimensional amorphous biopolymer that contains a great variety of bonds, of which approximately half are β-O-4 ether linkages [11]. These linkages are formed via biological lignification processes with three major monolignols serving as starting materials, namely *p*-hydroxyphenyl (**H**, from coumaryl alcohol), guaiacyl (**G**, from coniferyl alcohol) and syringyl (**S**, from sinapylalcohol) [2].

Because lignin is the only renewable resource that possesses an aromatic structure, it is considered to be an excellent candidate for the synthesis of bio-based polymers. Initially, researchers began to explore the direct valorization of lignin. Feldman et al. [12] developed a modified epoxy adhesive by directly blending epoxy resin with Kraft lignin. Comprehensive studies were conducted to gain insight into epoxy-lignin polyblend systems with regard to their curing kinetics, adhesive behavior, thermal properties, and structure-property relationships. It was found that blending 20% lignin with epoxy provided the ideal conditions for consolidation and thus offered the best performance. Kosbar et al. [13] evaluated several sources of lignin to develop a new series of bio-based epoxy resins. After co-reaction with di- or polyfunctional epoxies, resins possessing more than 50% lignin were successfully formulated. These blends were employed in various computer components, particularly printed wiring boards. Nonaka et al. [14] mixed an alkaline solution of industrial Kraft lignin with a water-soluble epoxy compound to develop a new resin system. This cured resin exhibited broad relaxation behavior and good dynamic mechanical properties.

Nevertheless, the direct utilization of lignin has presented significant challenges due to its large molecular weight and heterogeneity. Efforts to either blend lignin directly with commercial resins or to directly modify lignin with epichlorohydrin have been beset by difficulties due to poor efficiency of these processes and limitations with regard to the overall properties. Also, poor solubility as well as various electronic constraints and the steric hindrance effects presented by the functional groups of lignin have limited its applicability.

In recent years, various modification methods such as demethylation, phenolation, and hydroxymethylation have been introduced as effective pre-treatment strategies to enhance the reactivity and compatibility of raw lignin. Demethylation, a practical method to obtain lignin with additional free aromatic hydroxyl groups, has been studied by Chung et al. [15], Podschun et al. [16] and Song et al. [17] By reacting lignin with hydrobromide acid, indium triflate or iodocyclohexane, the methoxy groups in the 3 and 5 ring positions were substituted by hydroxyl groups, thus creating a pyrocatechol-like active moiety. Polyurethane resin and phenol formaldehyde adhesives were derived from demethylated lignin (DML) and were shown to offer competitive performance. Another modification strategy that has been employed to enhance the reactivity and applicability of lignin is phenolation. Yang et al. [18], Du et al. [19] and Podschun et al. [20] employed phenols to substitute aliphatic hydroxyl groups. The number of potential crosslinking sites provided by the introduced phenolic groups increased significantly under optimized reaction conditions. Based on these considerations, lignin-phenol-formaldehyde resin has become a predominant downstream product of phenolated lignin (PHL). Hydroxymethylation was investigated by Malutan et al. [21], Mansouri et al. [22] and Goncalves et al. [23]. Through reactions with formaldehyde and sodium hydrate, hydroxymethyl groups were introduced to lignin units, thus generating additional functional hydroxyl groups. Lignin-based polycondensation resins were developed with hydroxymethylated lignin (HML) for wood adhesives. In addition, other modification methods and lignin-based polymers have also been investigated, thus further adding to the viability of lignin as a feedstock for bio-based materials.

However, there have been no extensive investigations focusing on evaluations or comparisons of lignin-based epoxy resins that had been derived from the same original lignin feedstock but prepared via different modification methods. Furthermore, most works were concluded after a successful synthesis of the targeted resin without provided an in-depth subsequent exploration of the properties or applicability of the material. Few studies have explored the specific applications of lignin-based epoxy resins despite sporadic reports on the utilization of these materials in PCB boards or as anti-corrosion materials [24].

The objective of this work is to evaluate various types of modified lignin as precursors for the synthesis of lignin epoxy resin (LEP). In addition, new polymer grouting materials based on LEP were prepared as its innovative application. The LEP content and the structure of LEP employed were investigated as two key factors influencing the chemical and physical properties of lignin grouting resins. In order to achieve this goal, industrial grade organosolv lignin was first chemically modified and characterized. Subsequently, raw and modified lignin were reacted with epichlorohydrin in the presence of NaOH, which served as a catalyst. The effects of different conditions employed during this reaction and the post-treatment method were studied herein. Fourier-transform infrared spectroscopy (FTIR), nuclear magnetic resonance (NMR), and gel permeation chromatography (GPC) were used to characterize structural changes during the course of this synthesis and to demonstrate the success of our modification and epoxidation procedures. The compatibility of the obtained LEP was found to improve considerably under our optimized reaction conditions. The LEP was then employed as a precursor for new polymer grouting materials. Various mechanical tests such as tensile tests, compressive tests, bond tests, and shear tests were conducted on the cured lignin epoxy grouting resin, together with water absorption and corrosion resistance tests. In addition, the thermal properties of these samples were investigated via thermogravimetric analysis (TGA) and Differential Scanning Calorimeter (DSC). Scanning electron microscopy (SEM) images were used to characterize the morphologies of the cured grouting resin's fracture surface. Finally, with lignin's increasing availability as a by-product of the forestry industry, lignin epoxy grouting resin should offer various benefits due to its affordability, small environmental footprint, as well as its outstanding mechanical and thermal properties.

2. Experimental

2.1. Materials

Industrial grade organosolv lignin with a purity of 88% was obtained from Jinan Yang Hai Environmental Protection Material Co., Ltd. It was extracted from straw using a compound solvent, which was a mixture of ketone, alcohol and water, under the catalyzation of sulfuric acid. Prior to use, it was washed repeatedly with deionized water to remove any water-soluble impurities and then dried in a vacuum oven (2 h at 45 °C). Bisphenol A-type epoxy E-51 resin was purchased from China Petrochemical Co., Ltd. The E-51 resin, with its principal constituents being diglycidyl ether of bisphenol A, was a colorless transparent liquid with viscosity of 11–14 Pa·s at room temperature and epoxy value of 0.48–0.54 eq/mg. The structure of E-51 resin is show in Fig. 1.

XT epoxy curing agent was obtained from Guangzhou Chemical Grouting Co., Ltd., CAS. It was a kind of aliphatic polyamines modified by Mannich reaction, which possessed rich phenolic hydroxyl groups and novolac structures. However, its detailed formula was patented and

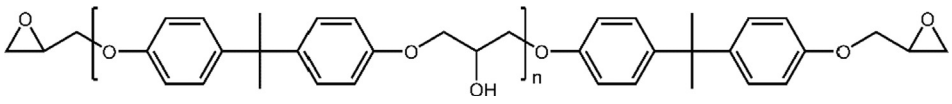

Fig. 1. The structure of E-51 epoxy resin.

has not yet been disclosed.

The following chemicals were obtained from commercial sources and used without further purification: Epichlorohydrin (ECH, Aladdin Reagent Co., Ltd.), 2,4,6-tris(dimethylaminomethyl)phenol (DMP-30, Aladdin Reagent Co., Ltd.), tetrabutylammonium bromide (TBAB, TCI), hexadecyltributylphosphonium bromide (TBHDPB, TCI), phenol (Tianjin Damao Chemical), formaldehyde solution (37%, Tianjin Damao Chemical), sodium hydroxide (Tianjin Damao Chemical), hydrobromic acid (48%, Aladdin Reagent Co., Ltd.), hydrochloric acid (37%, Guangzhou Chemical), sulfuric acid (98%, Guangzhou Chemical), dimethyl sulfoxide (DMSO, Aladdin Reagent), dimethylformamide (DMF, Aladdin Reagent Co., Ltd.), diethyl ether (Guangzhou Chemical), acetone (Guangzhou Chemical), and furfural (Aladdin Reagent Co., Ltd.).

2.2. Synthetic procedures

2.2.1. Demethylation

The demethylation of lignin was conducted using a well-established Lewis-acid-catalyzed method [15]. In summary, 30 g of purified raw lignin (RL) was thoroughly dissolved in 150 mL of DMF under vigorous stirring. Subsequently, 151.7 g of a 48% aqueous HBr solution and 0.9 g of TBHDPB were successively added. The reaction mixture was heated and stirred for 20 h at 110 °C. It was then cooled to ambient temperature and 700 mL of 1 M aqueous HCl solution was added in a dropwise manner. Precipitation occurred immediately and the mixture was stirred vigorously for 3 h. Subsequently, the heterogeneous solution containing the precipitate was filtered through a Brinell funnel to isolate the solid particles. A dark powder was recovered and dried in a vacuum oven overnight at 45 °C. For further purification, the powder was washed with diethyl ether to remove any soluble organic impurities. Finally, it was dried in a vacuum oven overnight at 45 °C again to obtain DML.

2.2.2. Phenolation

The phenolation of lignin was performed by reacting lignin with phenol directly in the presence of sulfuric acid, which served as a catalyst [20]. RL (30 g) was dissolved in 60 g of liquid phenol prior to the addition of 6.03 g of concentrated H_2SO_4. The homogenous mixture was heated and stirred for 1 h at 110 °C. Subsequently, this reaction was quenched with 450 g of acetone-H_2O (9:1) and precipitation was induced with 1500 mL of dilute H_2SO_4 (pH = 1). The precipitate was then recovered via centrifugation at 5000 rpm for 4 min. After this precipitate was repeatedly washed with warm water, it was dried in a vacuum oven overnight at 45 °C to obtain PHL.

2.2.3. Hydroxymethylation

Under the effect of formaldehyde and NaOH, hydroxymethyl groups were introduced into the lignin units [25]. To accomplish this, 30 g of RL was dissolved in 450 mL of 0.053 M NaOH solution and then 2.4 g of 37% formaldehyde solution was added. The alkaline reaction mixture was placed into a round bottom flask equipped with magnetic stirring rod and then heated to 50 °C for 8 h. Subsequently, a 1 M HCl solution was added dropwise into the mixture until its pH value reached 1. Brown solid particles appeared with the addition of the HCl, and these particles were then collected via centrifugation at 5000 rpm for 5 min. After repeated washing with deionized water and drying in a vacuum oven overnight at 45 °C, HML was finally obtained as a brown powder.

2.2.4. Epoxidation

A two-step epoxidation method was conducted by separating the ring-opening section of the epoxy groups from the ring-closing section. DMSO was introduced as an additional solvent to ensure the complete dissolution of the lignin. Practically speaking, 30 g of RL was dissolved into 300 g of DMSO, which was followed by the addition of 300 g of ECH and 3 g of TBAB. The homogeneous mixture was charged into a round-bottom flask and maintained at 70 °C for 3 h. The epoxy groups underwent ring-opening reactions during this stage. Subsequently, 60 g of NaOH solution (50%) was added into the mixture dropwise, and the epoxy rings were reconstructed. After this mixture was heated for another 1.5 h at 60 °C, a dark reaction mixture was obtained and a brown precipitate accumulated at the bottom of the flask. The mixture was rotary evaporated to remove the unreacted ECH and subsequently filtered to separate the liquid from the precipitate. The collected precipitate was washed repeatedly with water and then dried in a vacuum oven overnight at 45 °C. The obtained yellow-brown powder was denoted as RLEP-S and used for structural analysis. Meanwhile, the filtrate was poured into 1000 mL of deionized water, which resulted in the immediate precipitation of brown solid particles. This solid was collected via centrifugation at 5000 rpm for 4 min and then washed with water repeatedly prior to freeze-drying treatment. The resultant yellow powder was denoted as RLEP. DML, PHL, and HML were epoxidized via the same method as RLEP, and the corresponding products were denoted as DMLEP, PHLEP, and HMLEP, respectively.

2.2.5. Preparation of the chemical grouting materials

Various formulations of grouting materials were prepared from two components, which are denoted as A and B. The A component consisted of a matrix epoxy resin, LEP, and diluents, while the B component consisted of a curing agent and an accelerating agent. Epoxy resin E-51 was chosen as a matrix epoxy resin due to its excellent adhesive properties, low viscosity at room temperature, and its affordability. LEP of different content and different modifying types were introduced as replacements for petroleum-based epoxy resin, and their respective performances in this role were investigated. Furfural together with acetone was applied as a diluent, because they were able to reduce the viscosity of the resin significantly while enhancing the overall strength by forming interpenetrating polymer networks of furan resin. An XT amine curing agent was able to ensure the desired, rapid curing behavior at room temperature, although its detailed formula was patented and has not yet been disclosed. DMP-30, a widely used accelerating agent for epoxy resins, was used to adjust the curing speed and thus ensure that curing was achieved within a desirable timeframe. From an operational perspective, LEP was first dispersed in the hybrid diluent consisting of furfural and acetone to form a homogenous mixture. Epoxy resin E-51 was then added, and the mixture was stirred vigorously for a few minutes to obtain the A component, which was a homogenous dark liquid. The B component was prepared by thoroughly mixing a certain amount of XT curing agent with DMP-30. Subsequently, the A and B components were mixed and stirred thoroughly for at least 3 min. A homogeneous, dark liquid was finally obtained as the chemical grouting material. The formulations of prepared grouting materials regarding different LEP content and LEP types were shown in Table 1. The number in the sample codes was denoted as the weight in grams of lignin epoxy resin used in every 100 g E-51 resin.

2.3. Analytical procedures

2.3.1. FT-IR spectroscopy

FT-IR spectra of lignin and LEP were obtained using a typical KBr method with a Bruker Tensor 27 FT-IR spectrometer (Bruker, Billerica, MA, USA) after the samples had been purged with nitrogen. Each sample was scanned 16 times at a resolution of 1 cm^{-1} over the frequency range of 4000–600 cm^{-1}.

2.3.2. ^1H NMR spectroscopy

Lignin samples were acetylated in advance to enhance their solubility in organic solvents. Briefly, each 1 g lignin sample was added to a 16 mL mixture of pyridine and acetic anhydride (1:1, v/v). After stirring at ambient temperature for 48 h, the mixture was treated with 150 mL of 1% HCl at 0 °C. The resulting precipitate was filtered, washed with distilled water to a neutral pH, and then dried in a vacuum oven at

Table 1
Formulations of the prepared grouting materials.

Samples	A Component			B Component			
	E51 resin(g)	Furfural(g)	Acetone(g)	LEP Type	LEP(g)	Curing agent(g)	DMP-30(g)
RLEP-0	100	45	45	RLEP	0	20	1.25
RLEP-4	100	45	45	RLEP	4	20	1.25
RLEP-8	100	45	45	RLEP	8	20	1.25
RLEP-12	100	45	45	RLEP	12	20	1.25
RLEP-16	100	45	45	RLEP	16	20	1.25
DMLEP-16	100	45	45	DMLEP	16	20	1.25
PHLEP-16	100	45	45	PHLEP	16	20	1.25
HMLEP-16	100	45	45	HMLEP	16	20	1.25

40 °C. Finally, acetylated lignin was obtained as a black powder. Prior to the ^{1}H NMR analysis, approximately 0.1 g of acetylated lignin and approximately 0.01 g of *p*-nitrobenzaldehyde (which was used as an internal standard) [26], were dissolved thoroughly in DMSO-d_6. The ^{1}H NMR spectra were then recorded on a Bruker DRX-400 spectrometer (Bruker, Billerica, MA, USA).

2.3.3. GPC

The molecular weights and polydispersities of the lignin and LEP samples were determined by gel permeation chromatography (GPC). Calibration was performed using well-defined polystyrene standards. A Perkin-Elmer Series 200 HPLC system (Perkin-Elmer, Waltham, MA, USA), equipped with a Jordi Gel DVB column (Jordi Labs, Mansfield, MA, USA) was employed for this characterization. Lignin samples were also acetylated in advance and the characterization was conducted at 35 °C in tetrahydrofuran at a flow rate of 1 mL·min^{-1}.

2.3.4. SEM

Fracture surface morphologies of various cured grouting materials were observed using a FEI Quanta650 SEM (Thermo Fisher Scientific, Hillsboro, OR, USA) system. The fragments obtained after the tensile tests were stained on a copper grid with a conductive adhesive (gold) to enhance their conductivity prior to analysis.

2.3.5. TGA

Thermal stability was evaluated with a PerkinElmer TGA 4000 analyzer (Perkin-Elmer, Waltham, MA, USA) under a nitrogen flow (10 cm^3·min^{-1}). The samples (2–3 mg) were heated from 50 to 600 °C at a heating rate of 10 °C·min^{-1}. The weight loss and its first derivative weight were recorded simultaneously as a function of temperature.

The statistic heat-resistant index (T_s) was used to determine the thermal stability of the cured resins. This value was determined from the temperatures corresponding to a 5% weight loss ($T_{d5\%}$) and to a 30% weight loss ($T_{d30\%}$) from the sample, as measured via TGA. The T_s values were calculated via Eq. (1) [27]:

$$T_s = 0.49[T_{d5\%} + 0.6(T_{d30\%} - T_{d5\%})] \quad (1)$$

2.3.6. DSC

Differential Scanning Calorimeter analysis was conducted to investigate the effect of lignin epoxy resin content and lignin variants on the glass transition temperature (*Tg*) of the cured grouting resin with a Q2000 differential scanning calorimeter (TA Instruments, Newcastle, DE, USA). Cured grouting samples were massed (1–3 mg) and placed in aluminum sample pans (TA instruments). Two scans with a heating rate of 10 °C/min in a temperature range of 20–200 °C and a continuous nitrogen flow of 50 mL/min were done. The second scan was used for calculation of *Tg*.

2.3.7. Water absorption

Water absorption was measured by referring to ASTM D570-98. In detail, square specimens with a side length of 60 mm and a thickness of 1 mm were prepared. After dried in a vacuum oven over night, they were immersed in an excess amount of deionized water at room temperature for 48 h. The weight of the specimen before and after immersion were recorded as W_{dry} and W_{wet} respectively. The water uptake was calculated via Eq. (2), and the resultant values were reported as the average of three measurements.

$$\text{Wateruptake} = \frac{W_{wet} - W_{dry}}{W_{dry}} \times 100\% \quad (2)$$

2.3.8. Corrosion resistance

Corrosion resistance was studied by referring to ASTM D543-14. In detail, square specimens with a side length of 60 mm and a thickness of 1 mm were prepared. After dried in a vacuum oven over night, they were immersed completely in four kinds of chemical liquids, including 10% HCl, 10% NaOH, Toluene and Acetone, at room temperature for 7 d. The weight of the specimen before immersion were recorded as W_{before}. After the immersion, the specimen was dried in vacuum oven at 100 °C overnight and then their weight was recorded as W_{after}. The corrosion resistance was studied by calculating the mass loss ratio via Eq. (3), and the resultant values were reported as the average of three measurements.

$$\text{mass loss ratio} = \frac{W_{before} - W_{after}}{W_{before}} \times 100\% \quad (3)$$

2.3.9. Viscosity measurements

The viscosity of the mixed grouting material was measured with an NDJ-5S digital viscometer (Shanghai Precision and Scientific Instrument Corporation, Shanghai, China) by referring to ASTM D1084-08. The resultant values were reported as the average of three measurements.

2.3.10. Mechanical properties

Tensile tests, bond adhesion tests and shear tests by tension loading were conducted using a universal testing machine (Shenzhen Reger Instrument Co., Ltd, Guangdong, China) with a crosshead speed of 5 mm·min^{-1}. Meanwhile, the compressive tests were conducted using a TYE-2000 compressive testing machine (Wuxi Jianyi Experiment Instrument & Machinery Co., Ltd., Jiangsu, China). The mixed grouting material was poured into molds and cured at room temperature or used to bond separated specimens for 28 d prior to testing. The tensile tests were conducted in accordance with ASTM D638-14. In detail, dog bone-shaped molds were adopted and the prepared specimens (stretching zone width = 10 mm; thickness = 2 mm; and gauge length = 115 mm) were stretched. The bond tests were conducted by referring to ASTM C307-18. In detail, "∞"-shaped briquet specimens of cement-sand mortar (width at the waist of the briquet = 22.5 mm, depth of the briquet specimen = 22.2 mm) were made and first stretched into two separate fractions. After that, the two fractions were bonded using the prepared grouting resin and subsequently stretched to their breaking

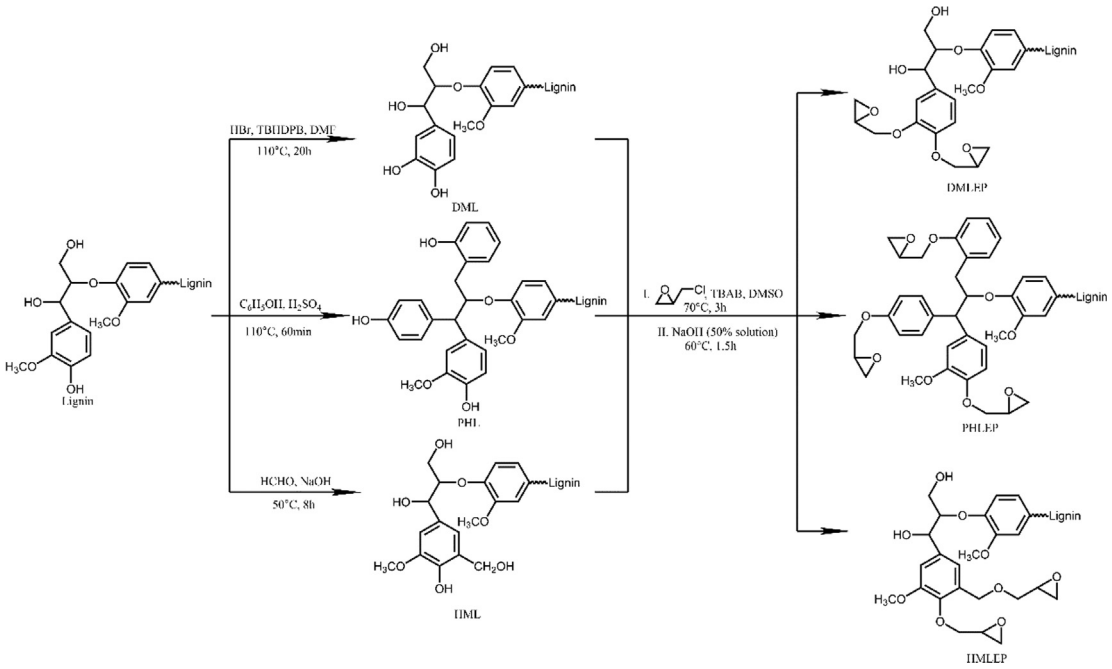

Scheme 1. Reaction pathway for the conversion of lignin to DML and PHL. Also shown is the subsequent conversion to DMLEP, PHLEP, and HMLEP.

points. The tensile strength of the bonded fractions was recorded according to ASTM C307-18 and was then denoted as the bond strength of the grouting resin. With regard to the shear tests by tension loading, they were conducted by referring to ASTM D1002-10. In detail, steel sheets (width = 25 mm, length of lapping area = 12.5 mm) were bonded and later stretched to their breaking points. Meanwhile, the compressive tests were conducted by referring to ASTM D695-15. In detail, cubic molds were employed for the compressive tests, and the prepared specimens (cubes with a side length of 18 mm) were compressed until they were completely crushed. The resultant values were reported as an average obtained from five measurements.

3. Results and discussion

3.1. Modification of lignin

Demethylation, phenolation, and hydroxymethylation are some of the most well-established modification methods to enhance the reactivity of lignin. The effectiveness of modified lignin as an epoxy resin precursor was evaluated in this work. As shown in Scheme 1, HBr, phenol, and formaldehyde were used as modifying agents to obtain DML, PHL and HML. During the demethylation process, the ether bonds of the methoxy groups in the 3 or 5 ring positions of lignin were expected to undergo cleavage in the presence of a Lewis acid catalyst. This approach was implemented via the reaction of RL in the presence of HBr, a phase-transfer agent (TBHDPB), and a water-DMF solvent mixture for 20 h at 110 °C. DML was finally collected via filtration and then purified and dried.

During the phenolation process, multiple phenolic reactive sites were introduced into the aromatic framework of the lignin. It was anticipated that this reaction would overcome the low reactivity and applicability of RL. In summary, RL was dissolved in and reacted with phenol under the catalysis of sulfuric acid at 110 °C for 1 h. PHL was collected via precipitation, centrifugation and finally by drying under vacuum. Hydroxymethylation was also implemented to introduce hydroxymethyl groups into the *ortho* positions of the aromatic rings of lignin. It was anticipated that this approach would effectively increase the number of reactive sites on the side-chains. RL, NaOH solution, and a formaldehyde solution were mixed together to form a homogeneous mixture that was kept at 50 °C for 8 h. HML was obtained after precipitation, filtration, purification, and subsequent drying under vacuum. In order to demonstrate that the lignin had been successfully modified, FT-IR and ^{1}H NMR spectroscopy were used to characterize the chemical structure and numbers of functional groups present before and after the modification. In addition, GPC was used to determine the changes in the molecular weight and the polydispersity.

As shown in Fig. 2, the FT-IR spectra of raw lignin and modified products were similar, which indicated that their skeletal structures remained unchanged. A broad band at ~3420 cm^{-1} was visible in all of the samples, which corresponded to the abundant hydroxyl groups in the phenolic and alcoholic structures of lignin. An intense band at 2935 cm^{-1} was attributed to C–H stretching in the methyl and methylene groups of the side-chains, while another band at 2854 cm^{-1} corresponded to C–H stretching in aromatic methoxy groups. An absorbance representing aromatic skeletal vibration was present at 1600 and 1508 cm^{-1}. Meanwhile, the absorption band at 1456 cm^{-1} was due to C–H bending vibrations of the methyl and methylene groups. The C–O stretching vibration corresponding to phenolic hydroxyl groups appeared at 1230 cm^{-1} and that of aliphatic hydroxyl groups

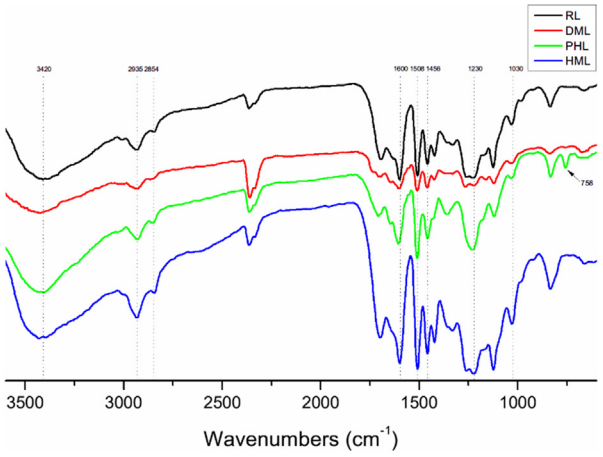

Fig. 2. The FT-IR spectra of RL, DML, PHL, and HML.

was visible at 1030 cm^{-1}. Although there may have been slight shifts in the band positions between RL and the various modified lignin derivatives (as will be described in greater detail below), the bands mentioned above were common among all of the lignin samples, and they were consistent with the structure of C_9 phenylpropanoid lignin units [28].

However, there were also some noticeable differences in the spectra of the modified products. In the spectra of DML, the main difference observed after demethylation was that the area of the peak corresponding to phenolic hydroxyl groups had increased while the area of that representing methoxy groups had decreased. This behavior was also observed in previous studies [29] and via NMR spectroscopy. In comparison between RL and PHL, the intensity of the O—H absorption peak at ~3415 cm^{-1} become higher in the spectrum of the latter than that in the former, which was due to the greater number of phenolic hydroxyl groups present after phenolation. The peak at 1030 cm^{-1} became weaker due to the replacement of C—O bonds at the Cα sites in RL by C—C bonds during the phenolation process. A new absorbance, detected at 758 cm^{-1} for PHL, was attributed to a C—H bending vibration in the *ortho*- or *para*-hydroxyphenyl groups. This result suggested that a condensation reaction had occurred between the substituents at the *ortho*- or *para*-positions in the phenol moieties and α-hydroxyl groups in the lignin side-chains [30]. Therefore, it was apparent the phenolation of lignin had taken place successfully.

In the spectra of the HML samples, the main bands remained in place after hydroxymethylation because there was neither an introduction of new functional groups nor loss of existing ones. Nevertheless, changes in the peak areas of the absorbance signals were observed. The peak areas of the signal corresponding to O—H stretching at ~3400 cm^{-1} and of those representing methylene groups at 2935 and 1456 cm^{-1} had all increased, which suggested that additional hydroxymethyl groups had been introduced into this lignin derivative. Meanwhile, an increase in the intensity at 1030 cm^{-1} also reflected the growth in the quantity of the hydroxymethyl groups [25].

Further characterization was implemented by studying the NMR spectra of RL and the modified lignin samples. All of the samples were reacted via pyridine-catalyzed acetylation with acetic anhydride prior to ^1H NMR characterization. This treatment suppressed hydrogen bonding so that the proton signals corresponding to the hydroxyl groups could be readily measured. The general spectra of each lignin sample shown in Fig. 3 were relatively similar, which suggested that the skeletal structure of the different lignin samples remained intact. An internal standard, *p*-nitrobenzaldehyde, was added as a reference to enable measurement of the functional group content. This standard was chosen because it possessed three key qualities: excellent miscibility, low volatility, and easily distinguishable proton signals. The peaks corresponding to *p*-nitrobenzaldehyde appeared at 10.15, 8.40, and 8.16 ppm, with the former signal belonging to the proton of the aldehyde group and the latter two representing those of the aromatic ring. Meanwhile, the protons of the acetoxy groups exhibited signals in in the range from 1.58 to 2.70 ppm. This spectral range could be further divided into the chemical sift range from 2.20 to 2.70 ppm for acetylated phenolic hydroxyl groups and from 1.58 to 2.20 ppm for acetylated aliphatic hydroxyl groups. The aromatic group protons in the lignin units were visible from 7.8 to 5.9 ppm. The signals observed in this spectral range did not change significantly before and after modification, which further demonstrated that the lignin possessed a stable skeletal structure. Proton signals in the range from 4.2 to 3.0 ppm corresponded to methoxy groups in lignin. Remarkable differences were observed in this spectral range, which indicated that the structure and functional group content changed during modification. After demethylation, the integrations of the methoxy group signals in the range at 4.2 to 3.0 ppm had decreased, thus demonstrating that the methoxy groups had been converted to hydroxyl moieties [15]. In addition, the intensity of the peak at 2.24 ppm increased slightly, indicating a growth in the aromatic acetyl group content in DML. Upon comparison of RL and PHL, the spectrum of the latter compound exhibited a dramatic increase in the signal integration at 2.23 ppm, while a decrease was observed at 1.92 ppm. This indicated a growth in the content of phenolic hydroxyl groups, which were converted from aliphatic moieties [21]. Furthermore, the intensity of peaks at ~7.0 ppm also increased, which was attributed to the growth in the number of aromatic rings. This was possibly due to the introduction of additional phenol groups to the lignin during the phenolation process. Regarding HML, an opposite change appeared. For example, the signal at ~1.98 ppm exhibited a significant increase in its integration after the hydroxymethylation process. This result demonstrated that more hydroxymethyl groups had been introduced into the lignin unit, reflecting the high reactivity of formaldehyde [25].

Further characterization was conducted through a quantitative NMR analysis method. According to previous work [31], the relative content of specific functional groups was calculated by comparing the signal integration for a given functional group proton with that of an internal standard. These measurements were performed via equation (4):

$$F = \frac{\frac{M}{I} \times A}{m} \times 100\% \tag{4}$$

where F denotes the relative content of specific functional groups; A represents the area of the peak that corresponds to the functional group in question; M denotes the weight of the internal standard (g); I is the area of the peak corresponding to the internal standard; and m denotes the weight of lignin (g). As seen in Fig. 3, the two peaks corresponding to the aromatic ring of *p*-nitrobenzaldehyde displayed similar intensities and areas. Their stability ensured that they provided a good reference for group content measurements. Thus, the mean value of the peak area at 8.40 and 8.16 ppm was chosen as an internal standard. The relative contents of methoxy, phenolic hydroxyl, and aliphatic hydroxyl groups as determined via these calculations are shown in Table 2.

As seen in Table 2, DML showed a decreased methoxy group content, as expressed by F in Eq. (4), from 1.65 in 1 g of lignin to 1.61 in 1 g of lignin. Meanwhile, the aromatic acetyl group content increased from 0.30 in 1 g of lignin to 0.40 in 1 g of lignin. A 10% increase in the total acetyl group content was discovered in DML in comparison with RL. Based on the mechanism of the acetylation reaction, phenolic and aliphatic hydroxyl groups were converted into aromatic and aliphatic acetyl groups in a one-to-one ratio. This ensured that the content of acetyl matched that of the hydroxyl groups. Thus, it was concluded that more phenolic hydroxyl groups were present in DML than in RL, and the total content of hydroxyl groups increased after demethylation at the same time. The above results confirmed that methoxy groups were converted into phenolic hydroxyl groups in the presence of HBr. Regrading PHL, a large amplification of the aromatic acetyl group content can be seen, from 0.30 in 1 g of lignin to 0.57 in 1 g of lignin. This result demonstrated that the hydroxyl group content increased significantly during the phenolation process. The aliphatic hydroxyl group content exhibited a modest decrease by 6%, indicating that phenolation occurred in some of the reactive sites where aliphatic hydroxyl groups were present. A slight diversification of the methoxy groups was also detected, which might be attributed to fragmentation of the polymeric lignin backbone. Successful phenolation was underlined by the changes mentioned above and introduced more potential reactive sites to lignin. Upon comparison of HML with RL, it can be seen that HML exhibited a higher aliphatic hydroxyl group content than that of RL, as the former was 0.81 in 1 g of lignin and the latter value was 0.63. This result indicated that more hydroxymethyl groups were introduced into lignin at various positions via different reaction mechanisms. Generally, the total hydroxyl group content increased significantly after all of the investigated modification strategies, with increases by 10%, 25% and 51% for DML, PHL, and HML, respectively. This would likely enhance the potential reactivity of these modified lignins towards lignin-derived

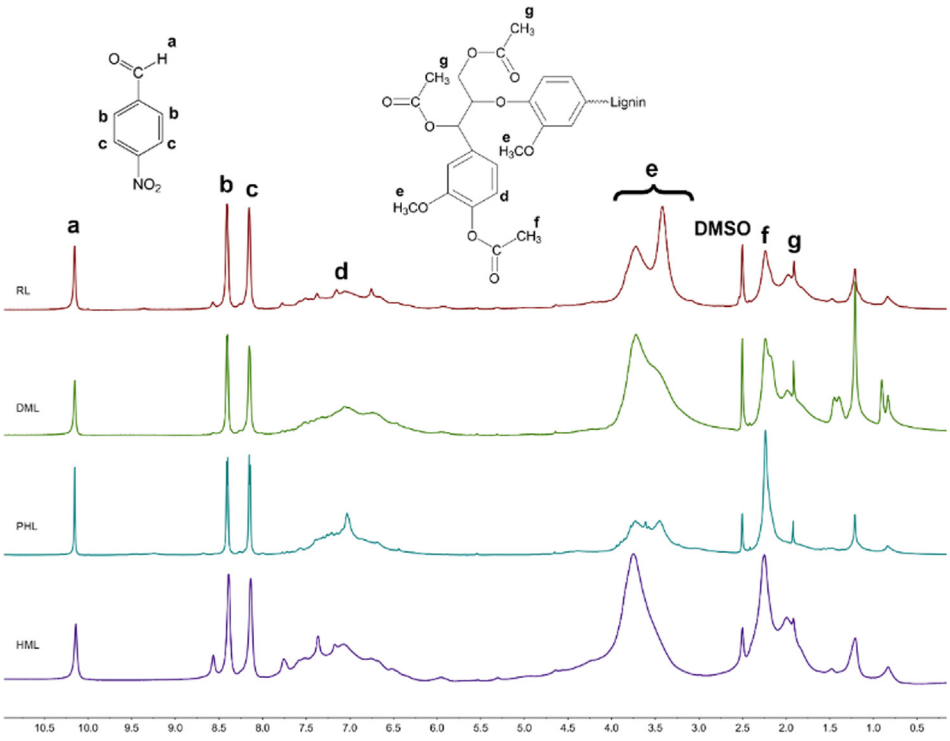

Fig. 3. The ^{1}H NMR spectra of RL, DML, PHL, and HML.

polymers, especially lignin epoxy resin.

The change in molecular weight and polydispersity between RL and the three types of modified lignins investigated herein were studied via GPC.

As shown in Table 3, RL was found to possess a relatively higher M_w than DML and PHL, which suggested that it possessed a more condensed structure. After demethylation, only a very slight fluctuation in the M_n and M_w was discovered. This may be demonstrated by Scheme 1 as only one single group participated in the reaction and the skeletal structure remained unchanged. A 17% decrease in M_w was found for PHL, which was also reported by Podschun et al. [20]. During acid catalyzed phenolation, substitution of the phenol group was often accompanied by cleavage of ether bonds among lignin units. Such side reactions yielded a smaller lignin backbone and led to a lower molecular weight. As for HML, the changes in both M_n and M_w were reversed. With a doubled M_n and 67% increase in the M_w, it can be deduced that condensation reactions occurred while the hydroxymethylation of lignin molecules was conducted. Decreases in the polydispersity were observed for all three of the modified samples. This shift may be attributed to distinct reactivity between the fractions with higher or lower molecular weights. Higher molecular weight lignin molecules tend to be more active under acid treatment and hence more readily cleaved (DML and PHL), but less likely to undergo condensation under alkali treatment (HML). In contrast, the lower

Table 3
Characterization of the molecular weights and polydispersities of RL, DML, PHL, and HML.

Sample	$\overline{M_n}$	$\overline{M_w}$	Polydispersity
RL	670	1001	1.49
DML	749	925	1.24
PHL	701	833	1.19
HML	1371	1670	1.22

Table 2
The Quantitative NMR analysis of RL, DML, PHL, and HML.

Sample	Mass of Sample (g)	Mass of internal standard (g)	Chemical shift (ppm)	8.40	8.16	4.00–3.00	2.49–2.20	2.20–1.60
			Proton assignment	Aromatic ring of *p*-nitrobenzaldehyde		Methoxy group	Aromatic acetate	Aliphatic acetate
RL	0.1147	0.0181	Integral area of chemical shifts & mean value	2.47 2.43	2.39	25.3	4.54	9.63
			Relative content in 1 g of lignin	0.16		1.65	0.30	0.63
DML	0.1034	0.0106	Integral area of chemical shifts & mean value	2.68 2.61	2.53	40.71	10.51	16.28
			Relative content in 1 g lignin	0.10		1.61	0.40	0.62
PHL	0.0963	0.0161	Integral area of chemical shifts & mean value	2.13 2.14	2.15	15.53	7.3	7.51
			Relative content in 1 g of lignin	0.17		1.21	0.57	0.59
HML	0.1392	0.0146	Integral area of chemical shifts & mean value	2.07 2.03	1.99	32.99	10.98	15.59
			Relative content in 1 g of lignin	0.11		1.71	0.59	0.81

molecular weight fraction was likely to remain stable after demethylation and phenolation, but have more opportunities to form new linkages in the presence of formaldehyde.

3.2. Epoxidation of lignin

In order to achieve better compatibility between lignin and matrix epoxy resin, lignin was further subjected to epoxidation reactions. In particular, epoxy groups were introduced into lignin units in the presence of ECH, a phase transfer catalyst, and NaOH. Through crosslinking reactions between the epoxy group and the curing agent, polymer networks were formed and thus better performance was anticipated over that available via direct blending. In the present study, a two-step method was investigated for the synthesis of lignin epoxy resin. By separating the ring-opening reaction of ECH from the following ring-closing reaction, products with low molecular weights and hence better solubility were synthesized. Briefly, RL was initially dissolved into an additional solvent, DMSO. ECH containing TBAB as a catalyst was then added to this solution. This mixture was heated at 70 °C for 3 h. During the above step, a ring-opening etherification reaction occurred between the hydroxyl groups of lignin and the epoxy groups of ECH, thus forming chloroalcohol ethers. Until this was achieved, the mixture remained homogeneous and clear. During the second step, the epoxy rings were reconstructed over a period of 1.5 h after the addition of NaOH. This ring-closing reaction resulted in the formation of a brown precipitate. Finally, RLEP-S and RLEP were obtained from the precipitate and the liquid, respectively, as described above.

FT-IR spectroscopy was used to characterize RLEP-S and RLEP. As shown in Fig. 4, an absorption peak corresponding to epoxide ring vibrations was observed at 910 cm^{-1} in the FT-IR spectrum of RLEP, which indicated successful epoxidation. In contrast, no such peaks were visible in the spectrum of RLEP-S. RLEP-S also exhibited a broader absorbance in comparison with other samples at 1020 cm^{-1}, which corresponded to aliphatic OH group vibrations. This may be explained by consumption of the epoxy groups during the crosslinking reaction, which formed ether bonds between lignin units and the released aliphatic hydroxyl groups [29].

Scheme 2 showed a possible self-condensation reaction between the unreacted lignin and LEP molecules. After the hydroxyl groups attacked the epoxy groups and formed new ether linkages, the degree of polymerization of lignin was therefore amplified. This resulted in an inflexible structure and finally in poor solubility.

The structures of DMLEP, PHLEP, and HMLEP were also confirmed by FT-IR spectroscopy. As shown in Fig. 4, all of the modified samples exhibited clearly visible signals at 910 cm^{-1}, thus providing evidence of epoxide ring vibrations and hence successful epoxidation. The bands at 1600 and 1508 cm^{-1} also remained stable, indicating that the samples possessed a robust aromatic backbone. Broad peaks near 3400 cm^{-1} were also present, but at a weakened intensity. This behavior was reasonable because not all of the hydroxyl groups were converted to epoxy groups. It was not possible to characterize RLEP-S via GPC due to its insolubility in common solvents. However, the molecular weights and polydispersities of the other LEPs were characterized by GPC.

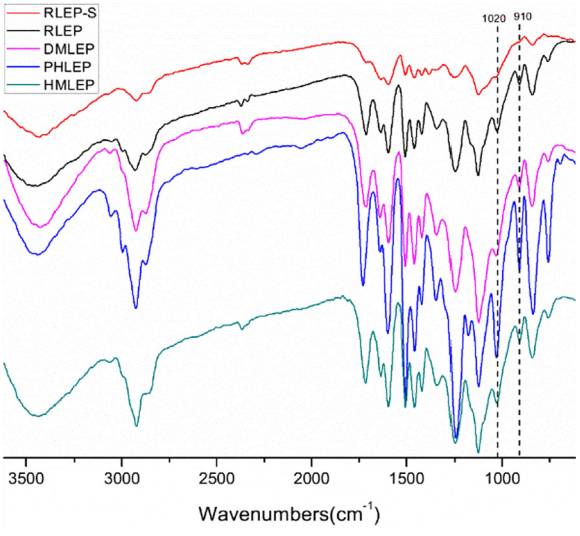

Fig. 4. FT-IR spectra of RLEP-S, RLEP, DMLEP, PHLEP, and HMLEP.

As shown in Table 4, all of the samples exhibited higher molecular weights after the epoxidation treatment, but in varying degrees. This indicated that lignin exhibited distinct reactivity towards epoxy group formation and also varying tendencies to undergo self-condensation when it was subjected to different modification techniques. RL was most likely to attack its epoxidized products and generate large molecules with a nearly seven-fold increase in M_w and a relatively large polydispersity of 1.96. DML showed a lower probability to undergo condensation, which was demonstrated by smaller multiples of molecular weight growth. After epoxidation, PHLEP exhibited the smallest M_n and M_w. These relatively low molecular weights were crucial for the physical state of PHLEP to remain liquid, though highly viscous. Better compatibility with other materials during mixing may also be achieved due to the modest molecular weight of this sample. Meanwhile, the polydispersity of HMLEP did not change, and the multiple of molecular weight growth with respect to that of the pristine lignin precursor was the lowest. This may be due to lower tendency toward self-condensation of aliphatic hydroxyl groups, which accounted for the majority of the hydroxyl groups in HML.

3.3. Effect of LEP content and structure on the rheological properties of the grouting materials

In the present work, RLEP was adopted as a representative sample to study the effect of the LEP content. The initial viscosity was recorded as the viscosity value immediately after the mixing of two components of epoxy grouting resin. In order to provide good fluidity and favorable permeation into small cracks, a low initial viscosity is necessary. The industry standard JC/T 1041-2007 has stipulated that the initial viscosity of an epoxy grouting resin should be lower than 30 mPa·s. Besides, grouting materials should not solidify too rapidly in case it cannot allow sufficient time for operation during construction processes. An operable time was set as the period between the mixing of two epoxy components and the time when the viscosity reached 200 mPa·s. According to the standard, the operable time should not be less than 30 min.

The data regarding the initial viscosity and operable time for samples with different RLEP content are listed in Table 5, while plots of the viscosity change over time with different RLEP content are shown in Fig. 5. It can be seen that samples with varying RLEP contents all maintained a relatively low initial viscosity in the range from 15 to 18 mPa·s, which were significantly lower than that of the industry standard (30 mPa·s). All of the grouts were homogenous mixtures and behaved as fluids. This was attributed not only to the good diluting effect of the furfural-acetone mixed dilution system, but also to the outstanding solubility and dispersity of RLEP in organic solvents. Because larger lignin molecules were introduced into the slurry for the RLEP-4 to RLEP-16 samples, a very slight increase in the initial viscosity was observed. Over time, the viscosity grew steadily in all of the samples. Divergence appeared after 2 h and became larger after 4 h. For RLEP-12, RLEP-8, RLEP-4, the viscosities observed at 5 h after mixing were lower than that of neat epoxy grouting resin (RLEP-0) in order of decreasing RLEP content. This may be deduced from relative abatement in the amount of curing agent, which became insufficient after RLEP addition and resulted in slower curing behavior. In contrast, as was the case for RLEP-16, the viscosity grew faster than that of RLEP-0. The

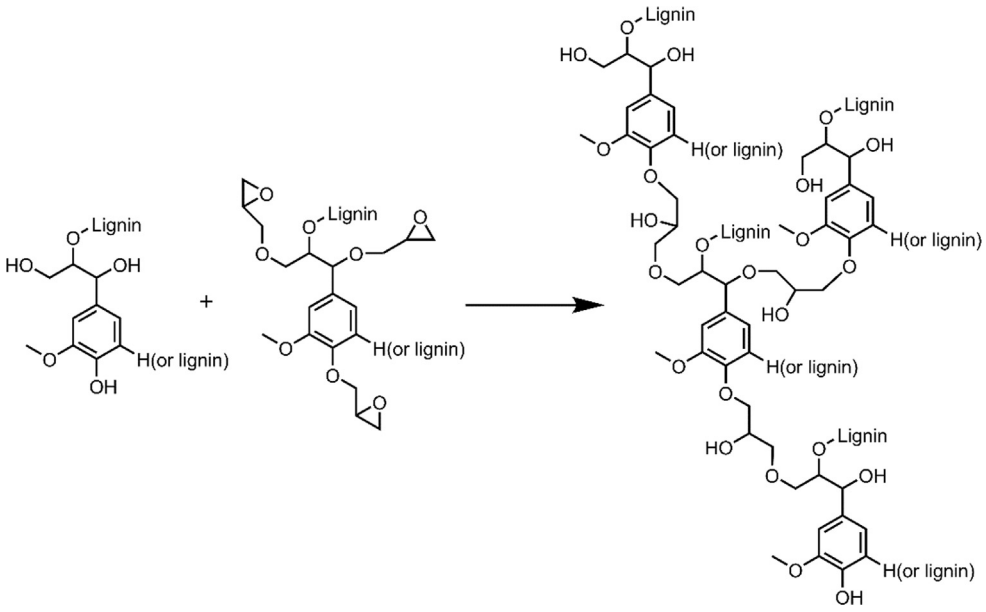

Scheme 2. Condensation reaction between lignin molecules.

Table 4
Characterization of molecular weight and polydispersity of RLEP, DMLEP, PHLEP, and HMLEP.

Sample	$\overline{M_n}$	Multiples of $\overline{M_n}$	$\overline{M_w}$	Multiples of $\overline{M_w}$	Polydispersity	Variation of PD
RLEP	3559	5.3	6979	7.0	1.96	+0.47
DMLEP	3026	4.0	3866	4.2	1.66	+0.42
PHLEP	2081	3.0	3100	3.7	1.49	+0.30
HMLEP	3666	2.7	4518	2.7	1.22	0

Table 5
Initial viscosities and operable times of grouting resins with different RLEP contents.

Samples	Initial viscosity (mPa·s)	Operable time (min)
RLEP-0	15	164
RLEP-4	19	181
RLEP-8	17	163
RLEP-12	18	161
RLEP-16	17	159

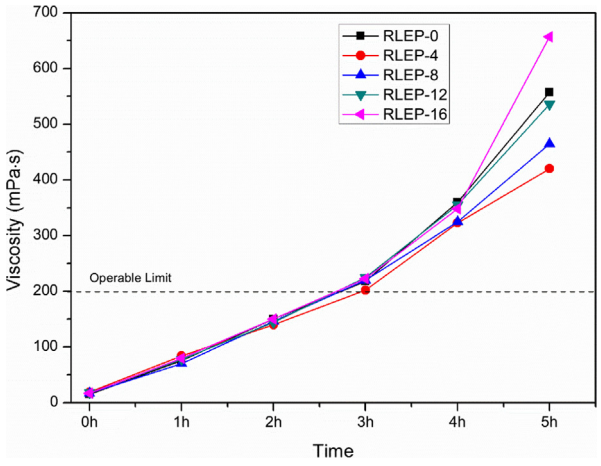

Fig. 5. Plots of the changes of viscosity over time for grouting resins with different RLEP contents.

large amount of hydroxyl groups introduced by RLEP may have been responsible for this behavior, due to their strong promotion of the crosslinking reaction between the epoxy groups and the amine curing agent. It can be deduced from the above results that the RLEP content reached a critical value at ~14%. At this point, the antagonistic effect and the accelerating effect of RLEP may have reached a balance.

In order to facilitate the replacement of petroleum-based epoxy resin with LEP to the greatest extent possible, a lignin epoxy resin content of 16% was employed for further studies. Table 6 shows the effect of different LEP types on the initial viscosities and operable times. Meanwhile, Fig. 6 depicts plots of the viscosity changes over time for samples incorporating different types of LEP. It can be seen that all of the samples possessed a qualified value of initial viscosity when the LEP content remained similar at 16%. However, that for DMLEP and HMLEP increased by 47% and 70% respectively. Such a densification may be attributed to the relatively poor compatibility between DMLEP, HMLEP, and the organic slurry because some visible insoluble particles remained present even after thorough stirring. A lower initial viscosity was achieved for PHLEP, mainly due to the fluidity of PHLEP and the resulting excellent miscibility. Various operable times were exhibited over the range from 61 to 152 min, and they also met the requirements. Therefore, the introduction of different types of LEPs provided a potential method to adjust the performance of grouting materials.

Distinct growth rates were discovered when the changes in viscosity were monitored over time. After the addition of DMLEP and HMLEP, the slurry grew viscous faster than was the case for that containing RLEP. This result was consistent with the trend regarding the initial viscosity, reflecting the thickening effect of LEP particles and the accelerating effect provided by abundant hydroxyl groups. After 5 h, the viscosity of HMLEP-16 had exceeded 3000 mPa·s while that of DMLEP-16 reached 1500 mPa·s. In contrast, the accelerating effect of PHLEP

Table 6
Initial viscosities and operable times for grouting resins with different types of LEPs.

Samples	Initial viscosity (mPa·s)	Operable time (min)
RLEP-16	17	159
DMLEP-16	25	93
PHLEP-16	13	152
HMLEP-16	29	61

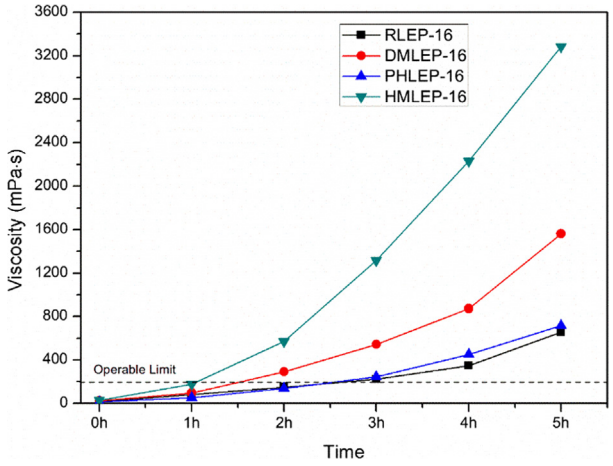

Fig. 6. Plots of the changes in viscosity over time for grouting resins with different LEP variants.

was not apparent during the first 5 h, and even a slight retardation in the viscosity growth was detected prior to 2 h. This behavior revealed that the phenolic hydroxyl groups in PHLEP were less reactive compared with those in HMLEP and DMLEP.

3.4. Effect of LEP content and variants on the mechanical properties of the grouting materials

Tensile tests, compressive tests, and adhesion tests were conducted to evaluate several key factors of the grouting material. According to the industry standard, cured epoxy grouting resin should possess high tensile and compressive strength to ensure mechanical stability. Good bonding strength was also required to ensure stable adhesion of concrete cracks. Specifically, the tensile strength should be at least 10 MPa, while the compressive strength should be greater than 40 MPa, and the bond strength should be more than 3.0 MPa. In addition, shear tests via tension loading were performed to assess the adhesion of the grouting resin onto steel surfaces. The results of the shear tests provided an index reflecting the adhesion of the grouting resins from another perspective, but could vary due to differences in the matrix metal and surface treatment. Therefore, there was no uniform standard for shear strength. In the mechanical tests, RLEP was also selected as a representative to study the effect of the resin composition.

The results of the tensile tests on epoxy grouting resins with different RLEP contents are shown in Table 7. After the introduction of 4 g RLEP into 100 g E51 resin (to obtain RLEP-4), the tensile strength diminished by 39%. Although the tensile strength increased slightly from this value when the RLEP amount was 8 g (for RLEP-8), it reached even lower values as the RLEP content was increased to 12 g and 16 g (for RLEP-12 and RLEP-16, respectively). Three factors were associated with this declination. Firstly, the introduction of RLEP caused second-phase islands to form during the curing process, which behaved as defects and compromised the stability of the structure. Secondly, RLEP behaved a plasticizer and exhibited negative effects on the crosslinking density of the matrix material. Thirdly, RLEP may have damaged the continuity and integrity of the epoxy network near lignin molecules, and thus lowered the strength of this material. The Young's modulus increased by 24% with an RLEP content of 8 g, which was accompanied by a 5% decrease in the elongation at break. This behavior demonstrated the positive effect of RLEP on the brittleness and stiffness of the resin. As the RLEP content reached 16 g, reductions in the strength, modulus and elongation at break were all observed. The small second-phase islands mentioned above may have been the main cause for this behavior, resulting in a premature catastrophic failure.

Table 7
Results of tensile tests on epoxy grouting resins with different RLEP contents.

Sample	Tensile Strength (MPa)	Young's Modulus (GPa)	Elongation at Break (%)
RLEP-0	36.56 ± 1.60	0.63 ± 0.19	4.04 ± 0.54
RLEP-4	22.41 ± 3.72	0.42 ± 0.16	3.07 ± 0.41
RLEP-8	24.52 ± 2.88	0.78 ± 0.24	3.84 ± 0.43
RLEP-12	19.88 ± 3.24	0.69 ± 0.57	3.77 ± 0.36
RLEP-16	19.20 ± 1.83	0.46 ± 0.11	3.89 ± 0.35

Similar changes were generally observed during the evaluations of the compressive strength. In contrast with the tensile strength, the overall trend was smooth, and it only diminished by 21% from that of the neat epoxy resin when the RLEP content was 16 g. It was likely that the weakening effect of the tiny defects within the cured grouting resin was diminished under pressure. The declination may primarily have been caused by the lower crosslinking density that resulted from by the higher LEP content. However, it was noteworthy that despite this reduction, the tensile strength and the compressive strength of the lignin epoxy grouting resin were still far beyond the minimum industry standard, exceeding those values by 1.92- and 2.55-fold, respectively.

As for the bond strength, grouting resin samples with different RLEP content exhibited similar values. It must be noted that patterns regarding the failure of each sample corresponded to a cohesive failure rather than an adhesion failure. This was an important consideration, and it indicated that the strength of the cured grouting resin had exceeded that of the cement mortar block. Thus, it can be concluded that all of the samples exhibited bond strengths in excess of 3.0 MPa, and they thus fully met the industry standard.

The shear strength by tension loading was also used to study the adhesion performance to a steel surface. In Fig. 7c, the shear strength decreased by 32% after the addition of 8 g RLEP. This may have been due to the increasing viscosity of the epoxy resin following the curing treatment and thus poor adhesion to the steel surface. However, a 9% growth was observed when the RLEP content reached 16 g, as the anchoring effect between lignin molecules and the steel surface became stronger with the incorporation of more RLEP molecules. After complete evaluation of the mechanical properties, it was found that the prepared grouting materials with RLEP contents up to 16 g in 100 g E51 epoxy resin readily met the industry standard, which thus demonstrated their potential for industrial applications.

In order to maximize the amount of petroleum-based epoxy resin that can be replaced by lignin epoxy resin, a content of 16 g in 100 g E51 epoxy resin was adopted to investigate the performance of different LEP variants. As shown in Table 8 and Fig. 8, the use of different types of LEP led to wide variations in the performances during the mechanical tests. As for DMLEP-16, a 30% enhancement in the tensile strength was observed, together with a slight reduction of the Young's modulus and an increase in the elongation percentage with respect to its RLEP counterpart. This indicated that the demethylation of lignin during the initial phase had a positive effect on both the elasticity and strength of this material. The greater number of functional groups in the DMLEP-16 sample may have created more connections between lignin molecules and the matrix epoxy network, thus resulting in a higher crosslinking density and fewer defects. Meanwhile, the DMLEP-containing grouting resin exhibited competitive performance with regard to its compressive strength, bond strength, and shear strength, making it a better candidate than RLEP. Both PHLEP-16 and HMLEP-16 exhibited similar behavior during the tensile tests, showing a moderate increase in the tensile strength and a 15% decrease in the Young's Modulus. This revealed that replacing RLEP with PHLEP or HMLEP provided more elasticity to the cured resin. However, considering their improved performances during the compressive tests and shear tests, it was possible that the effects of PHLEP and HMLEP may have resulted from different mechanisms. With a 9% increase in compressive strength and a 17% growth in the shear strength, PHLEP provided the grouting resin with an overall improvement in performance. This can be explained by

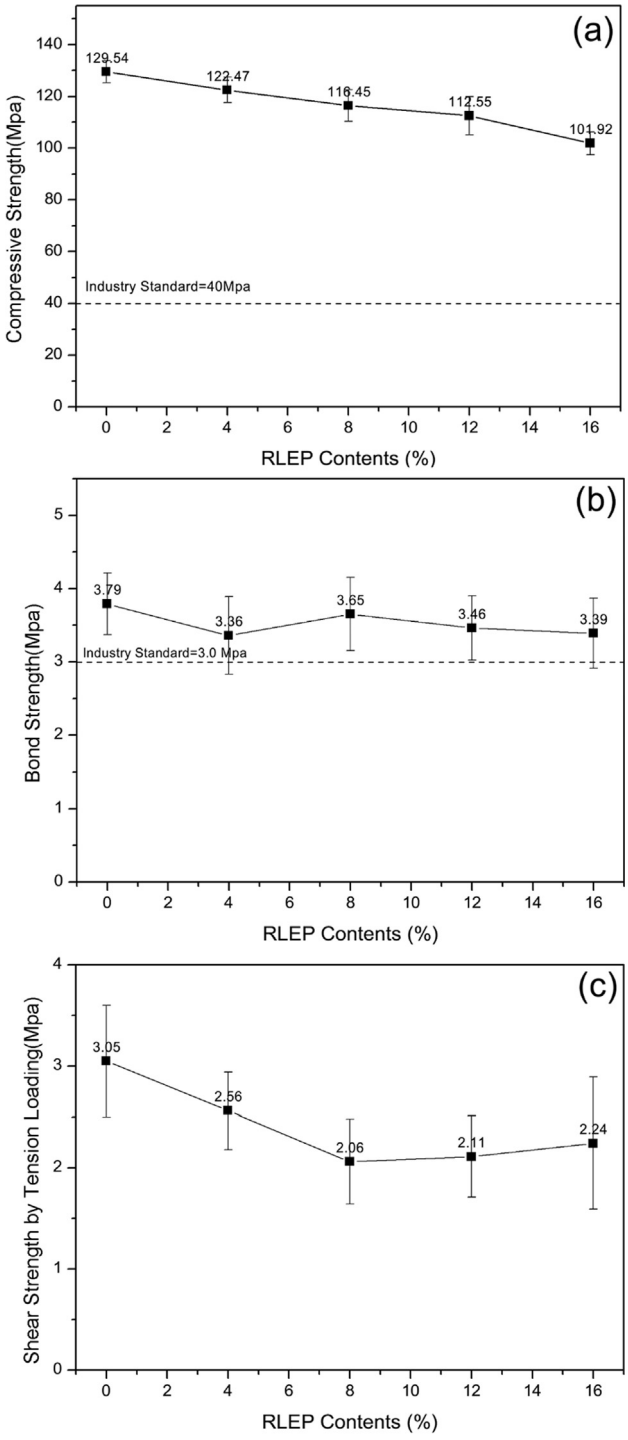

Fig. 7. Data obtained from (a) compressive tests, (b) bond tests, and (c) shear tests by tension loading on samples with different RLEP content.

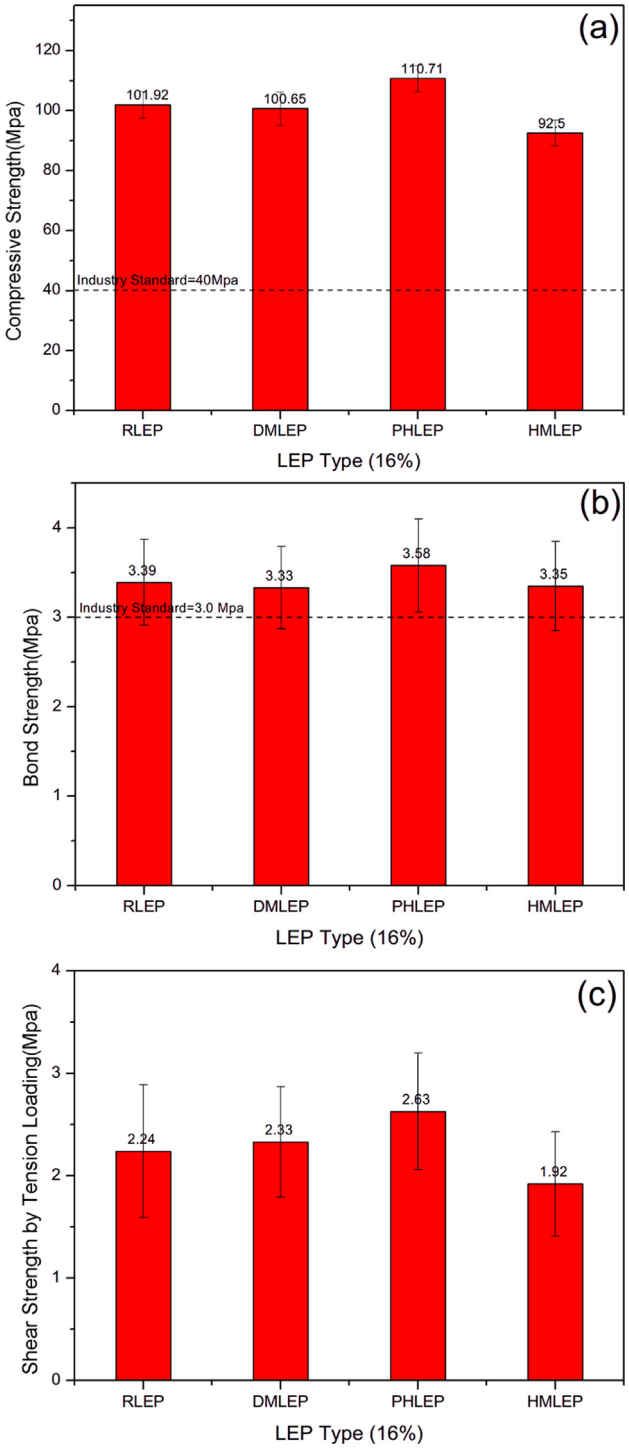

Fig. 8. Results of (a) compressive tests, (b) bond tests, and (c) shear tests by tension loading with different LEP types.

Table 8
Results of tensile tests on epoxy grouting resin samples incorporating different LEP variants.

Sample	Tensile Strength (MPa)	Young's Modulus (GPa)	Elongation at Break (%)
RLEP-16	19.20 ± 1.83	0.46 ± 0.11	3.89 ± 0.35
DMLEP-16	24.99 ± 3.25	0.41 ± 0.12	5.46 ± 0.94
PHLEP-16	21.60 ± 1.45	0.39 ± 0.16	4.29 ± 0.10
HMLEP-16	20.53 ± 2.44	0.38 ± 0.08	4.44 ± 0.28

its extraordinary compatibility with the matrix material, high functional group content, and rigid molecular structure. With the introduction of more phenol groups, the lignin molecules had stronger crosslinks with the epoxy network, which inhibited the formation of defects. In contrast, the incorporation of HMLEP resulted in a slight decline in both the compressive and shear strength. This can be reasonably deduced from the poor miscibility and wettability of HMLEP. Through a comprehensive evaluation of the DMLEP-16, PHLEP-16, and HMLEP-16 epoxy grouting resins, it should be noted that all three types of these materials fully satisfied the afore-mentioned industry standard.

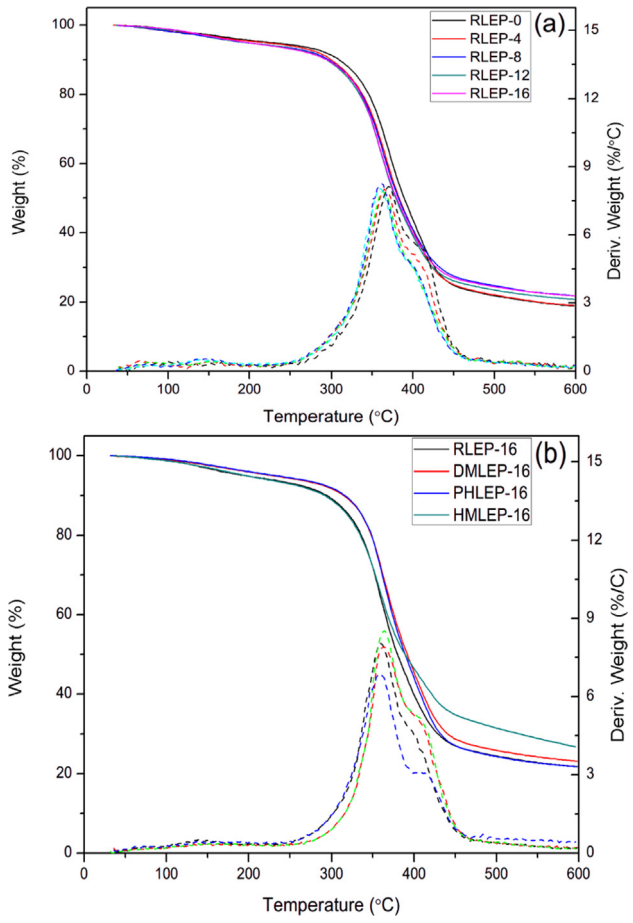

Fig. 9. TG and DTG curves of grouting resins with (a) different RLEP contents and (b) different LEP types.

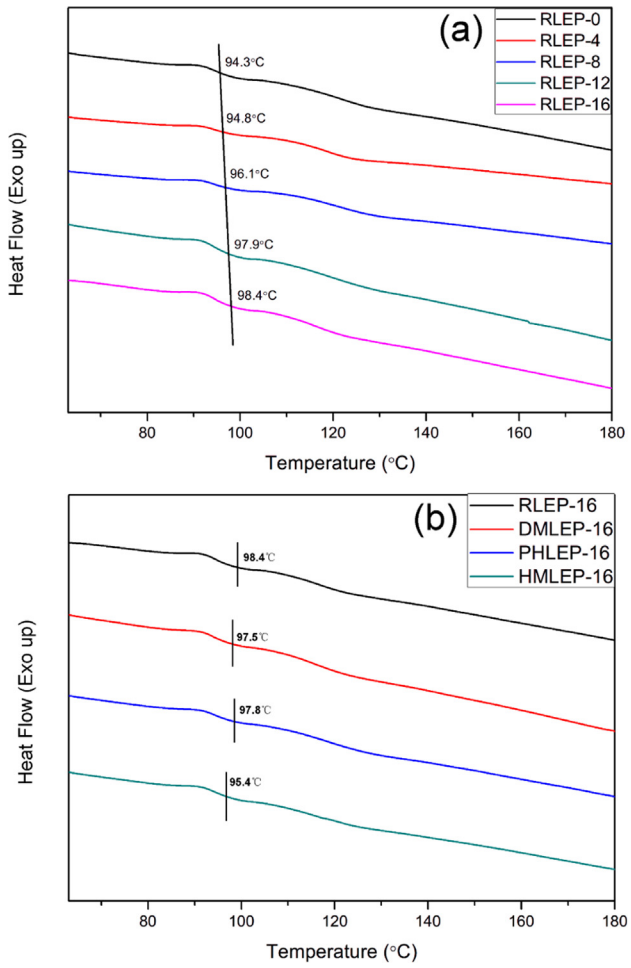

Fig. 10. The DSC curves of cured grouting resins with (a) different RLEP contents and (b) different LEP types.

Table 9
Thermal properties of the cured lignin grouting resins.

Samples	$T_{d5\%}$ (°C)	$T_{d30\%}$ (°C)	R_{600} (%)	T_s
RLEP-0	225.3	362.8	18.9	150.8
RLEP-4	217.5	355.0	19.1	147.0
RLEP-8	194.0	354.0	21.9	142.1
RLEP-12	195.8	352.5	20.8	142.0
RLEP-16	196.1	351.4	21.8	141.7
DMLEP-16	228.5	362.3	23.1	151.3
PHLEP-16	231.9	361.2	21.8	151.6
HMLEP-16	199.1	352.2	26.8	142.5

Considering the different circumstances for various applications, as well as the load-bearing conditions, and raw material availability in practice, grouting resins with different LEP variants can thus be chosen that best accommodate a given requirement. For instance, DMLEP can be used in grouting resins for cracks that are vulnerable to stretching, PHLEP can be employed to strengthen defects that may be subject to compression, and HMLEP could be used if formaldehyde is readily available.

3.5. Effect of LEP content and variants on the thermal properties of the grouting materials

Thermogravimetric analysis (TGA) was used to investigate the thermal stability and degradation behaviors of the cured lignin epoxy grouting resins. The TGA curves recorded under nitrogen for samples with different RLEP contents and LEP variants are shown in Fig. 9. Meanwhile, the values of the degradation temperatures at 5% ($T_{d5\%}$) and 30% ($T_{d30\%}$) weight loss, the residual weight percentage at 600 °C (R_{600}) and the values of statistic heat-resistant index (T_s) are presented in Table 9.

As seen from Fig. 9 and Table 9, cured grouting resins that incorporated RLEP had a slightly lower $T_{d5\%}$ (217.5 to 194.0 °C) than their RLEP-free counterpart (RLEP-0, 225.3 °C), and this temperature remained stable after RLEP content had reached 8 g in 100 g E51 epoxy resin. The $T_{d30\%}$ values of all grouting resins that incorporated RLEP exhibited a decrease 7–10 °C in comparison with that of RLEP-0. Comparing the T_s of RLEP-0 with that if the RLEP-containing materials, a reduction of up to 6% was observed for the latter samples. These changes reflected a lowered thermal stability of the lignin grouting resins, which was possibly due to the presence of more thermally degradable lignin molecules [27] and readily cleavable ether bonds. However, such a degradation was negligible in practice.

With regard to the grouting resins incorporating different types of lignins, their thermal properties were found to vary. The DMLEP-16 and PHLEP-16 samples showed comparable $T_{d5\%}$, $T_{d30\%}$ and thus T_s values to those of neat epoxy resin (RLEP-0), which had improved from that of RLEP-16. The increased number of functional groups and the resultant stronger bonding with the matrix material may have been the main cause of this behavior. No significant changes were observed for HMLEP-16 in comparison with RLEP-16, indicating that hydroxymethylation had little effect on the final thermal properties.

Differential Scanning Calorimeter (DSC) analysis was also conducted to study the effect of lignin content and lignin variants on the glass transition temperature (*Tg*). Prior to tests, the grouting resins were cured at room temperature for 28d to simulate a complete solidification

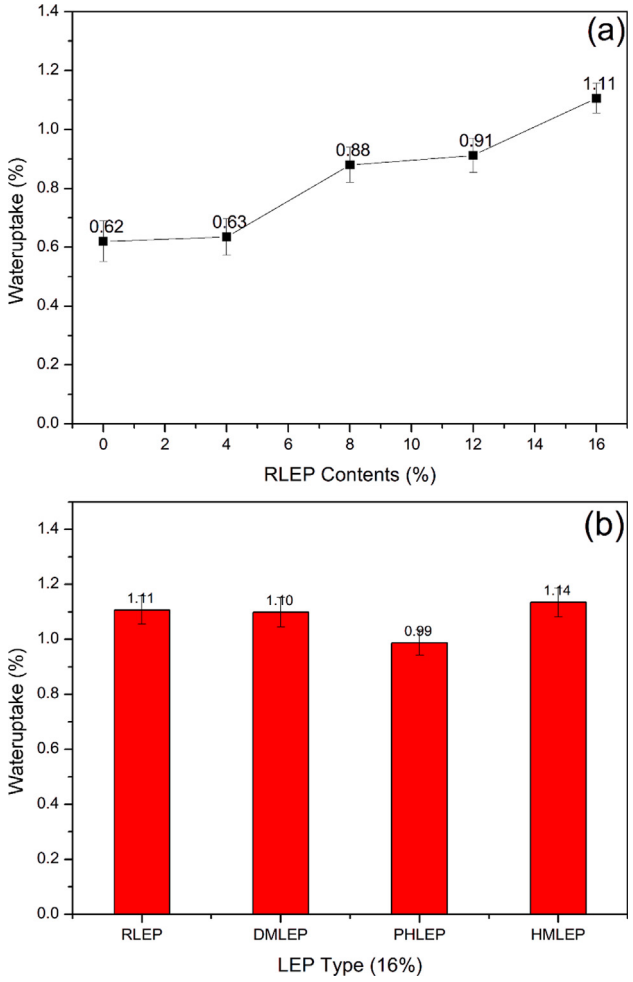

Fig. 11. The water absorption behavior of grouting resins with (a) different RLEP contents and (b) different LEP types.

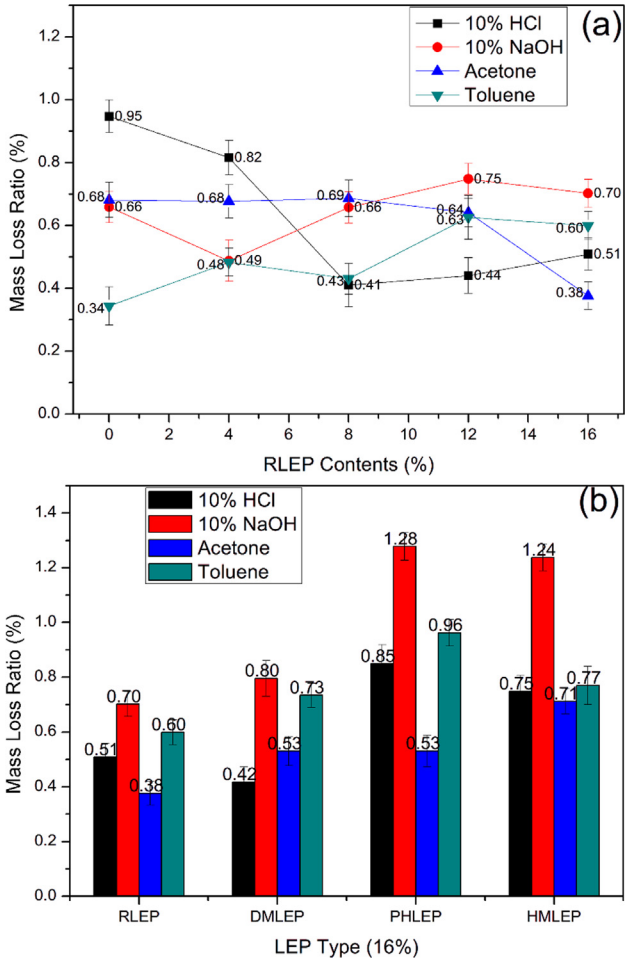

Fig. 12. . The corrosion resistance performance of grouting resins with (a) different RLEP contents and (b) different LEP types.

in actual construction. The DSC curves with different RLEP contents and different LEP types were shown in Fig. 10.

As shown in Fig. 10(a), *Tg* went through a slight and monotonic increase after the introduction of RLEP, from 94.3 °C to 98.4 °C. This may come from a higher crosslinking density brought by more lignin molecules. Considering the abundant hydroxyl groups and epoxy groups of lignin, it was very likely for lignin to play a positive role of crosslinker between matrix networks. Also, due to possible inhomogeneous dispersion and resulted rigid proportion, *Tg* can also be affected to a higher level. As for samples with different LEP types, some difference was seen from Fig. 10(b). Compared with RLEP, grouting resins with HMLEP displayed a lower *Tg*. This was reasonable as hydroxymethylation brought more flexible hydroxymethyl side chain groups to lignin units, which made the overall structure looser. Meanwhile, DMLEP and PHLEP maintained a similar *Tg* with RLEP, partially because of the moderate change of the overall structure by these modification methods.

In general, all the samples exhibited higher *Tg* and even much higher thermal degrading temperature than the usual working temperature of grouting materials according to the results of DSC and TGA. This made the promise that the prepared grouting reins were able to work effectively at application scenarios with high temperature.

3.6. Water absorption

Fig. 11 illustrated the water absorption behavior of cured grouting resins with different LEP content and different LEP types. It can be seen from Fig. 11(a) that the water uptake of cured grouting resin experienced a gradual growth as the RLEP contents went higher, from 0.62% in neat epoxy resin to an almost doubled 1.11% when RLEP content reached 16%. This was probably because of the incompact and discontinuous structure brought by more large lignin molecule, which created hollow cavities that left more space to be occupied by water. Regarding grouting resins with different LEP types in Fig. 11(b), very similar performance with RLEP were detected from DMLEP and HMLEP. This can be well explained by much the same microstructure as shown in SEM images. An 11% decrease was found for PHLEP. This may result from its outstanding miscibility as well as smooth and continuous internal structure, which provided less void space for water storage. Seen from a macro point of view, however, all the samples exhibited a very small level of water absorption, reflecting their compact structure after fine curing and indicating their promising application in waterproofing projects.

3.7. Corrosion resistance

The corrosion resistance performances of grouting resins were thoroughly studied as it is very likely for corrosion from acid, base and organic solvents to occur during applications like seepage prevention. Four typical liquids, including 10% HCl, 10% NaOH, acetone and toluene were selected to simulate possible corrosive media and the corresponding resistance performance were reflected by the mass loss ratio after sufficient immersion of samples. As shown in Fig. 12(a), the prepared lignin grouting resins exhibited varying corrosion performance towards different liquids and with different RLEP contents. Broadly

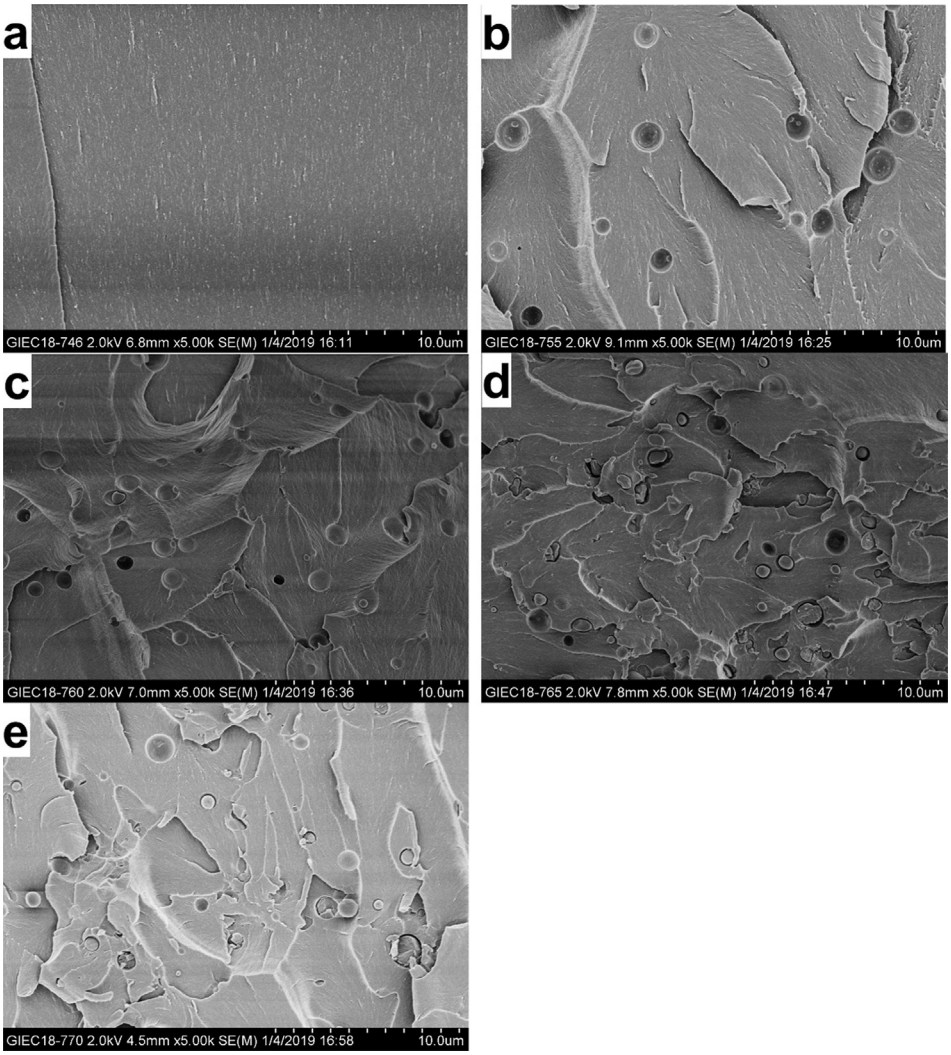

Fig. 13. SEM images of fracture surfaces of grouting resins with various RLEP contents: (a) RLEP-0, (b) RLEP-4, (c) RLEP-8, (d) RLEP-12, and (e) RLEP-16.

speaking, resistance to acid and acetone became stronger as more lignin were incorporated, which was probably because lignin molecules brought more rigid connection to the resin network. When suffering base solution and toluene, the weight loss ratio basically remained unchanged with different RLEP content, displayed a compact combination between lignin and epoxy matrix which prevent solvent molecules from taking effect. In terms of different LEP types, PHLEP exhibited a highest mass loss ratio from almost all four kinds of chemical liquids. This was likely to result from the high reactivity brought by higher hydroxyl groups content. DMLEP and HMLEP stayed the same with RLEP, also shown low vulnerability towards corrosion from chemical reagents. Seen from an absolute level, however, all the samples possessed a less than 1.3% weight loss ratio after being immersed in various chemical liquids, which reflected their outstand corrosion resistance performance. This meant that the prepared lignin grouting resins were able to work reliably in typical corrosive environments.

3.8. Morphological analysis

The fractured surfaces of cured lignin epoxy grouting resins were studied by SEM. As shown in Fig. 13, increases in the LEP content resulted in remarkable differences in the morphologies. Although phase separation was not distinctly observed during the preparation of the slurry at the beginning, crater-like features became visible after the introduction of RLEP. In Fig. 13(a), the fracture surface of RLEP-0 was smooth and homogeneous, thus demonstrating the uniform structure of the neat epoxy resin. After the addition of RLEP, flaws appeared in varying degrees. In Fig. 13(b) and (c) (for RLEP-4 and RLEP-8, respectively), only sporadically distributed crater-like features were discovered, which may have compromised the integrity of the epoxy network and then caused a weakening in the mechanical properties. As the RLEP content increased, the density of craters also grew. As shown in Fig. 13(d) and (e), concentrated lignin particles, as well as large hollow cavities were discovered for RLEP-12 and RLEP-16, respectively. Several causes may have accounted for this phenomenon. Firstly, despite the homogeneity at the initial stage, dissolved RLEP began to shrink and separate from the matrix as the curing process continued. This was probably due to loss of the solvent from the slurry [32], which was caused by either evaporation under the exothermic effect of the curing reaction or due to the furfural-acetone system undergoing condensation reactions. Secondly, RLEP tended to form a firm mixture with the epoxy matrix when the temperature increased during the curing progress, but the cleavage of bonds and phase separation would occur during the cooling of the matrix due to thermal stresses induced by the differences in the coefficients of thermal expansion. Thirdly, when the epoxy matrix and RLEP were subjected to external forces, they tended to exhibit different strengths and moduli, causing cracks and fractures to occur at their point of interaction.

The fracture images of cured lignin epoxy grouting resin samples incorporating different types of LEPs exhibited similar patterns. Crater-

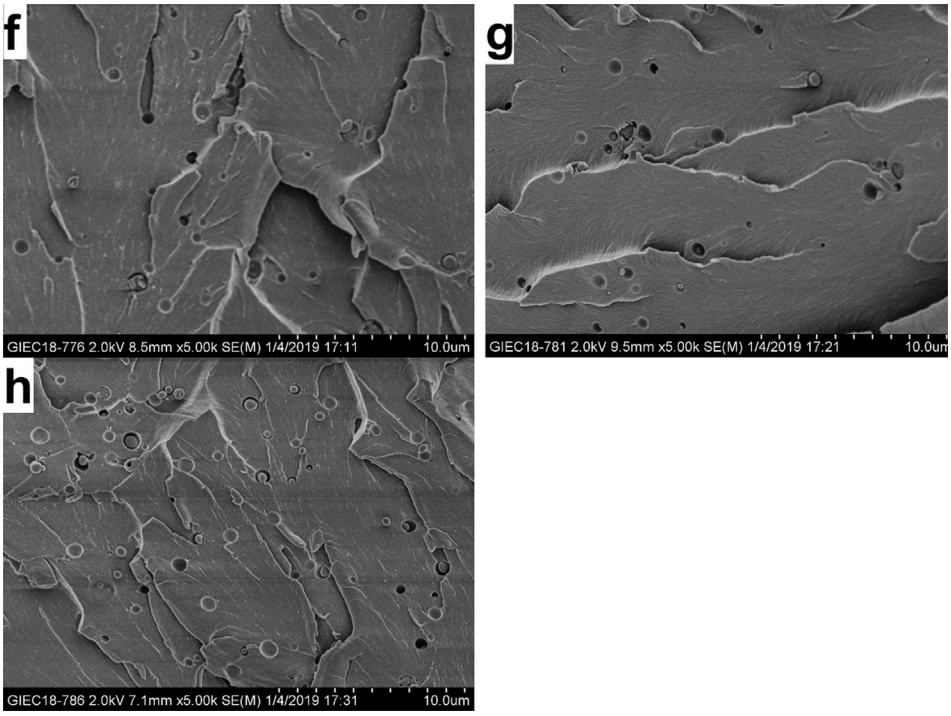

Fig. 14. SEM images of fracture surface of grouting resins with different RLEP types, including: (f) DMLEP-16, (g) PHLEP-16, and (h) HMLEP-16.

like features accompanied by clustered lignin particles were observed. However, their density and number varied significantly. In Fig. 14(f), the DMLEP-16 sample exhibited a better ordered fracture compared with its RLEP-16 counterpart. Only a few sphere-shaped lignin particles were visible, and the crater-like features were also sporadic. This may be explained by the greater number of functional groups in DML and thus better compatibility with the matrix material. As for PHLEP, the fracture in Fig. 14(g) was far flatter than those found in the other samples. The density of small crater-like features was also lower. This was consistent with the good miscibility of PHLEP with the matrix. As mentioned earlier, PHLEP remained in a liquid state rather than forming solid particles, which thus yielded a homogenous mixture during both the preparation and the curing process. This also resulted in the improved mechanical performance of the PHLEP grouting resin. In contrast, a large number of lignin spheres and collapsed hollow cavities were visible in Fig. 14(h) for HMLEP. From the initial stage of the grouting resin preparation, HMLEP showed poor solubility in organic solvents. During the curing process, it tended to self-aggregate and form small clusters. This was partially due to the increased molecular weight as well as the wettability. Therefore, it was also reasonable that HMLEP possessed relatively poor mechanical performance.

4. Conclusions

Lignin was successfully incorporated into chemical grouting materials in the present work. The prepared lignin epoxy grouting resin showed outstanding properties with RLEP content reaching up to 16%. It had a low initial viscosity (17 mPa·s) and good mechanical properties (19.20, 101.92 and 3.39 MPa for tensile, compressive, and bond strength, respectively), and they greatly surpassed the industry standard. Also, they were thermal stable, waterproofing and chemically resistance. Demethylation, phenolation, and hydroxymethylation treatment were able to increase the functional group contents and thus effectively enhance the final mechanical and thermal performance. The DMLEP-containing samples had a 30% improvement in the tensile strength and 6.8% enhancement of the heat-resistance, and thus they would be suitable for applications in which they would be subjected to stretching and high temperatures. The PHLEP-containing resin had a lower initial viscosity and better miscibility due to its liquid-like nature, indicating its potential applicability in scenarios where fluidity is strictly required. Meanwhile, the HMLEP-containing material maintained good performance and exhibited the fastest curing behavior, and it thus may be well-suited for urgent repair applications requiring rapid adhesion performance. Overall, lignin has displayed great potential as a replacement for petroleum-based materials in the preparation of high-performance chemical grouting materials.

Notes

The authors declare no competing financial interest.

Acknowledgement

We are grateful for the financial support from The National Key Research and Development Program of China (2017YFD0601003) and GDAS' Project of Science and Technology Development (2018GDASCX-0807).

References

[1] Q. Zhou, J.P. Hao, P. Lv, J.J. Men, Study on a new adhesive of concrete cracks repairing, Adv. Mater. Res. 168–170 (2010) 1308–1312, https://doi.org/10.4028/www.scientific.net/AMR.168-170.1308.
[2] C. Asada, S. Basnet, M. Otsuka, C. Sasaki, Y. Nakamura, Epoxy resin synthesis using low molecular weight lignin separated from various lignocellulosic materials, Int. J. Biol. Macromol. 74 (2015) 413–419, https://doi.org/10.1016/j.ijbiomac.2014.12.039.
[3] C. Aouf, H. Nouailhas, M. Fache, S. Caillol, B. Boutevin, H. Fulcrand, Multi-functionalization of gallic acid. Synthesis of a novel bio-based epoxy resin, Eur. Polym. J. 49 (6) (2013) 1185–1195, https://doi.org/10.1016/j.eurpolymj.2012.11.025.
[4] R. Zhou, W. Cheng, Y. Feng, H.Y. Wei, F. Liang, Y. Wang, Interactions between three typical endocrine-disrupting chemicals (EDCs) in binary mixtures exposure on myocardial differentiation of mouse embryonic stem cell, Chemosphere 178 (2017) 378–383, https://doi.org/10.1016/j.chemosphere.2017.03.040.
[5] C. Voirin, S. Caillol, N.V. Sadavarte, B.V. Tawade, B. Boutevin, P.P. Wadgaonkar, Functionalization of cardanol: towards biobased polymers and additives, Polym. Chem. 5 (9) (2014) 3142–3162, https://doi.org/10.1039/c3py01194a.
[6] M. Chrysanthos, J. Galy, J.-P. Pascault, Preparation and properties of bio-based epoxy networks derived from isosorbide diglycidyl ether, Polymer 52 (16) (2011)

3611–3620, https://doi.org/10.1016/j.polymer.2011.06.001.
[7] S. Benyahya, C. Aouf, S. Caillol, B. Boutevin, J.P. Pascault, H. Fulcrand, Functionalized green tea tannins as phenolic prepolymers for bio-based epoxy resins, Ind. Crops Prod. 53 (2014) 296–307, https://doi.org/10.1016/j.indcrop.2013.12.045.
[8] H. Hosney, B. Nadiem, I. Ashour, I. Mustafa, A. El-Shibiny, Epoxidized vegetable oil and bio-based materials as PVC plasticizer, J. Appl. Polym. Sci. 135 (20) (2018), https://doi.org/10.1002/app.46270.
[9] D. Feldman, D. Banu, M. Khoury, Epoxy lignin polyblends.3. Thermal-properties and infrared-analysis, J. Appl. Polym. Sci. 37 (4) (1989) 877–887, https://doi.org/10.1002/app.1989.070370403.
[10] B.M. Upton, A.M. Kasko, Strategies for the conversion of lignin to high-value polymeric materials: review and perspective, Chem. Rev. 116 (4) (2016) 2275–2306, https://doi.org/10.1021/acs.chemrev.5b00345.
[11] R. Auvergne, S. Caillol, G. David, B. Boutevin, J.P. Pascault, Biobased thermosetting epoxy: present and future, Chem. Rev. 114 (2) (2014) 1082–1115, https://doi.org/10.1021/cr3001274.
[12] D. Feldman, D. Banu, C. Luchian, J. Wang, Epoxy lignin polyblends - correlation between polymer interaction and curing temperature, J. Appl. Polym. Sci. 42 (5) (1991) 1307–1318, https://doi.org/10.1002/app.1991.070420514.
[13] L.L. Kosbar, J. Gelorme, Biobased epoxy resins for computer components and printed wiring boards, Proceedings of the 1997 Ieee International Symposium on Electronics and the Environment - Isee-1997, San Francisco, 1997, pp. 28–32.
[14] Y. Nonaka, B. Tomita, Y. Hatano, Synthesis of lignin/epoxy resins in aqueous systems and their properties, Holzforschung. 51 (2) (1997) 183–187, https://doi.org/10.1515/hfsg.1997.51.2.183.
[15] H. Chung, N.R. Washburn, Improved lignin polyurethane properties with Lewis acid treatment, ACS Appl. Mater. Interfaces 4 (6) (2012) 2840–2846, https://doi.org/10.1021/am300425x.
[16] J. Podschun, B. Saake, R. Lehnen, Catalytic demethylation of organosolv lignin in aqueous medium using indium triflate under microwave irradiation, React. Funct. Polym. 119 (2017) 82–86, https://doi.org/10.1016/j.reactfunctpolym.2017.08.007.
[17] Y. Song, Z. Wang, N. Yan, R. Zhang, J. Li, Demethylation of wheat straw alkali lignin for application in phenol formaldehyde adhesives, Polymers. 8 (6) (2016) 209, https://doi.org/10.3390/polym8060209.
[18] S. Yang, J.-L. Wen, T.-Q. Yuan, R.-C. Sun, Characterization and phenolation of biorefinery technical lignins for lignin–phenol–formaldehyde resin adhesive synthesis, RSC Adv. 4 (101) (2014) 57996–58004, https://doi.org/10.1039/c4ra09595b.
[19] X. Du, J. Li, M.E. Lindström, Modification of industrial softwood kraft lignin using Mannich reaction with and without phenolation pretreatment, Ind. Crops Prod. 52 (2014) 729–735, https://doi.org/10.1016/j.indcrop.2013.11.035.
[20] J. Podschun, B. Saake, R. Lehnen, Reactivity enhancement of organosolv lignin by phenolation for improved bio-based thermosets, Eur. Polym. J. 67 (2015) 1–11, https://doi.org/10.1016/j.eurpolymj.2015.03.029.
[21] T. Malutan, R. Nicu, V.I. Popa, Contribution to the study of hydroxymetylation reaction of alkali lignin, BioResources. 3 (1) (2008) 13–20.
[22] N.E.E. Mansouri, A. Pizzi, J. Salvado, Lignin-based polycondensation resins for wood adhesives, J. Appl. Polym. Sci. 103 (3) (2007) 1690–1699, https://doi.org/10.1002/app.25098.
[23] A.R. Goncalves, P. Benar, Hydroxymethylation and oxidation of Organosolv lignins and utilization of the products, Bioresour. Technol. 79 (2) (2001) 103–111, https://doi.org/10.1016/s0960-8524(01)00056-6.
[24] J. Ding, Epoxidation modification of renewable lignin to improve the corrosion performance of epoxy coating, Int. J. Electrochem. Sci. (2016) 6256–6265.
[25] N.-E. El Mansouri, Q. Yuan, F. Huang, Synthesis and characterization of kraft lignin-based epoxy resins, BioResources. 6 (3) (2011) 2492–2503.
[26] J. Li, J. Zhang, S. Zhang, Q. Gao, J. Li, W. Zhang, Fast curing bio-based phenolic resins via lignin demethylated under mild reaction condition, Polymers 9 (12) (2017) 428, https://doi.org/10.3390/polym9090428.
[27] S. Ma, X. Liu, L. Fan, Y. Jiang, L. Cao, Z. Tang, J. Zhu, Synthesis and properties of a bio-based epoxy resin with high epoxy value and low viscosity, ChemSusChem. 7 (2) (2014) 555–562, https://doi.org/10.1002/cssc.201300749.
[28] K. Sawamura, Y. Tobimatsu, H. Kamitakahara, T. Takano, Lignin functionalization through chemical demethylation: preparation and tannin-like properties of demethylated guaiacyl-type synthetic lignins, Acs Sustain. Chem. Eng. 5 (6) (2017) 5424–5431, https://doi.org/10.1021/acssuschemeng.7b00748.
[29] A. Jablonskis, A. Arshanitsa, A. Arnautov, G. Telysheva, D. Evtuguin, Evaluation of Ligno Boost™ softwood kraft lignin epoxidation as an approach for its application in cured epoxy resins, Ind. Crops Prod. 112 (2018) 225–235, https://doi.org/10.1016/j.indcrop.2017.12.003.
[30] Z. Liu, X. Lu, L. An, C. Xu, A novel cationic lignin-amine emulsifier with high performance reinforced via Phenolation and Mannich reactions, BioResources. 11 (3) (2016) 6438–6451, https://doi.org/10.15376/biores.11.3.6438-6451.
[31] J. Li, W. Wang, S. Zhang, Q. Gao, W. Zhang, J. Li, Preparation and characterization of lignin demethylated at atmospheric pressure and its application in fast curing biobased phenolic resins, RSC Adv. 6 (71) (2016) 67435–67443, https://doi.org/10.1039/c6ra11966b.
[32] G.P. Mendis, I. Hua, J.P. Youngblood, J.A. Howarter, Enhanced dispersion of lignin in epoxy composites through hydration and mannich functionalization, J. Appl. Polym. Sci. 132 (1) (2015), https://doi.org/10.1002/app.41263.